

Syracuse University

**SURFACE**

---

Physics

College of Arts and Sciences

---

7-29-2014

## Electron and hole drift mobility measurements on thin film CdTe solar cells

Qi Long

*Syracuse University*

Steluta A. Dinca

*Syracuse University*

Eric A. Schiff

*Syracuse University*

Ming Yu

*First Solar, Inc*

Jeremy Theil

*First Solar, Inc.*

Follow this and additional works at: <https://surface.syr.edu/phy>



Part of the [Condensed Matter Physics Commons](#)

---

### Recommended Citation

Long, Qi; Dinca, Steluta A.; Schiff, Eric A.; Yu, Ming; and Theil, Jeremy, "Electron and hole drift mobility measurements on thin film CdTe solar cells" (2014). *Physics*. 516.

<https://surface.syr.edu/phy/516>

This Article is brought to you for free and open access by the College of Arts and Sciences at SURFACE. It has been accepted for inclusion in Physics by an authorized administrator of SURFACE. For more information, please contact [surface@syr.edu](mailto:surface@syr.edu).

## Electron and hole drift mobility measurements on thin film CdTe solar cells

Qi Long, Steluta A. Dinca, E. A. Schiff, Ming Yu, and Jeremy Theil

Citation: [Applied Physics Letters](#) **105**, 042106 (2014); doi: 10.1063/1.4891846

View online: <http://dx.doi.org/10.1063/1.4891846>

View Table of Contents: <http://scitation.aip.org/content/aip/journal/apl/105/4?ver=pdfcov>

Published by the [AIP Publishing](#)

---

### Articles you may be interested in

[Copper-doped CdTe films with improved hole mobility](#)

Appl. Phys. Lett. **91**, 092113 (2007); 10.1063/1.2778455

[Hole current impedance and electron current enhancement by back-contact barriers in CdTe thin film solar cells](#)

J. Appl. Phys. **100**, 124505 (2006); 10.1063/1.2400799

[Simulated admittance spectroscopy measurements of high concentration deep level defects in CdTe thin-film solar cells](#)

J. Appl. Phys. **100**, 033710 (2006); 10.1063/1.2220491

[Lock-in thermography and nonuniformity modeling of thin-film CdTe solar cells](#)

Appl. Phys. Lett. **84**, 729 (2004); 10.1063/1.1645322

[Cathodoluminescence of Cu diffusion in CdTe thin films for CdTe/CdS solar cells](#)

Appl. Phys. Lett. **81**, 2962 (2002); 10.1063/1.1515119

---



**AIP** | Journal of  
Applied Physics

*Journal of Applied Physics* is pleased to  
announce **André Anders** as its new Editor-in-Chief

## Electron and hole drift mobility measurements on thin film CdTe solar cells

 Qi Long,<sup>1</sup> Steluta A. Dinca,<sup>1</sup> E. A. Schiff,<sup>1</sup> Ming Yu,<sup>2</sup> and Jeremy Theil<sup>2</sup>
<sup>1</sup>Department of Physics, Syracuse University, Syracuse, New York 13244-1130, USA

<sup>2</sup>First Solar, Inc., 1035 Walsh Ave, Santa Clara, California 95050, USA

(Received 14 May 2014; accepted 13 July 2014; published online 29 July 2014)

We report electron and hole drift mobilities in thin film polycrystalline CdTe solar cells based on photocarrier time-of-flight measurements. For a deposition process similar to that used for high-efficiency cells, the electron drift mobilities are in the range of  $10^{-1}$ – $10^0$   $\text{cm}^2/\text{V s}$ , and holes are in the range of  $10^0$ – $10^1$   $\text{cm}^2/\text{V s}$ . The electron drift mobilities are about a thousand times smaller than those measured in single crystal CdTe with time-of-flight; the hole mobilities are about ten times smaller. Cells were examined before and after a vapor phase treatment with  $\text{CdCl}_2$ ; treatment had little effect on the hole drift mobility, but decreased the electron mobility. We are able to exclude bandtail trapping and dispersion as a mechanism for the small drift mobilities in thin film CdTe, but the actual mechanism reducing the mobilities from the single crystal values is not known. © 2014 AIP Publishing LLC. [<http://dx.doi.org/10.1063/1.4891846>]

Thin film polycrystalline cadmium telluride solar modules are now manufactured in large quantities, and the conversion efficiency of the best cells has recently surpassed 20%.<sup>1</sup> Nonetheless, rather little is known about their photocarrier mobilities, which are crucial parameters for understanding the optoelectronic properties of materials and devices.<sup>2,3</sup> More than 25 yr ago, Takahashi *et al.* reported electron drift mobilities of 15–25  $\text{cm}^2/\text{V s}$  in diodes based on electrochemically deposited films of CdTe.<sup>4</sup> This is well below typical values of about  $10^3$   $\text{cm}^2/\text{V s}$  reported for single crystals of CdTe.<sup>5–8</sup> Hall effect measurements on thin films also give fairly low mobilities, but an analysis of photo-Hall measurements incorporating grain boundaries yielded an intra-grain electron mobility of  $3 \times 10^2$   $\text{cm}^2/\text{V s}$ .<sup>9</sup> This latter value was proposed for thin film CdTe solar cell modeling in one paper.<sup>10</sup>

In this Letter, we report direct time-of-flight measurements of the photocarrier drift mobilities in thin film CdTe solar cells prepared at First Solar. Photocarrier transit times across the cells were as large as hundreds of nanoseconds. For cells with higher open-circuit voltages ( $V_{OC}$ ), the electron drift mobilities range from  $10^{-1}$ – $10^0$   $\text{cm}^2/\text{V s}$ , and the hole mobilities range from  $10^0$ – $10^1$   $\text{cm}^2/\text{V s}$ . For reference, we note that typical hole mobilities reported in single crystals are around  $10^2$   $\text{cm}^2/\text{V s}$ .<sup>5</sup> These results are summarized in Fig. 1, where we show the correlation of electron and hole drift mobilities for the thin film CdTe cells we have measured and also for single crystals as reported in the literature.<sup>5–8</sup> In the figure, the solid black symbols represent thin-film cells that did not receive a vapor phase  $\text{CdCl}_2$  treatment and thus had markedly lower open-circuit voltages. These cells have larger electron drift mobilities than the treated cells, which is an unexpected finding.

In solar cells with large carrier mobilities, mobilities affect the useful thickness of a cell mainly through the minority carrier diffusion length. Low carrier mobilities give rise to additional effects on solar cells. As one example, the depletion width of a film is significantly reduced by solar photo-generation levels when carrier mobilities are low,<sup>11</sup> and we have seen evidence for this effect in photocapacitance

measurements on CdTe cells similar to those used for the present work.<sup>12</sup> Additionally, grain boundary recombination has been proposed as limiting the open-circuit voltage in thin-film CdTe cells. For low mobility materials, such recombination is likely to be “diffusion limited”, in which case the recombination time is inversely proportional to the minority carrier mobility.<sup>13,14</sup> The effect of vapor phase treatment, which increased the open-circuit voltages of our cells while reducing the electron drift mobility, is consistent with this expectation.

Six coupons of CdTe solar cells were made at First Solar for these experiments. Each coupon has 16 cells. We have included a layer diagram in Fig. 1, which shows the semi-transparent back contacts that are needed for electron drift-mobility measurements. The typical transmittance of this back contact is 0.3 at wavelengths from 500–800 nm.

We summarize properties for the six coupons in Table I. Coupons 1–4 were deposited using the same process; coupon

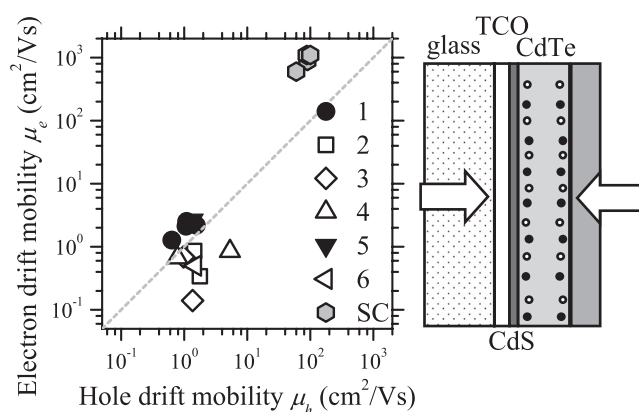


FIG. 1. The drawing illustrates the main layers of the bifacial solar cells used for the measurements. Top illumination (660 nm wavelength) generates photocarriers near the CdS/CdTe interface, and bottom illumination generates photocarriers near the metal/CdTe interface. The graph shows the correlation of the electron and hole drift mobilities in single crystals (SC),<sup>5–8</sup> as well as a summary of the present measurements on thin-film CdTe. The different symbols indicate the six different coupons; solid symbols are for untreated coupons. Detail measurements for all six coupons are shown in Table I.

TABLE I. Coupon details.

Coupon	Treat	$V_{oc}$ (V)	$\mu_h$ ( $\text{cm}^2/\text{V s}$ )	$\mu\tau_{h,t}$ ( $\text{cm}^2/\text{V}$ )	$\mu_e$ ( $\text{cm}^2/\text{V s}$ )	$\mu\tau_{e,t}$ ( $\text{cm}^2/\text{V}$ )
1	No	0.48	0.6	$3.0 \times 10^{-7}$	1.3	$3.9 \times 10^{-7}$
2	Yes	0.69	1.4	$2.5 \times 10^{-6}$	0.9	$2.2 \times 10^{-7}$
3	Yes	0.75	1.4	$2.6 \times 10^{-7}$	0.1	$2.1 \times 10^{-7}$
4	Yes	0.73	0.8	$1.2 \times 10^{-6}$	0.7	$2.2 \times 10^{-7}$
5	No	0.54	1.4	$5.8 \times 10^{-7}$	2.6	$1.1 \times 10^{-6}$
6	Yes	0.80	1.5	$3.8 \times 10^{-6}$	0.5	$2.2 \times 10^{-7}$

1 had no post-deposition treatment, and 2–4 have varying treatments with vapor-phase  $\text{CdCl}_2$ . Coupons 5 and 6 were prepared using a somewhat different process; coupon 5 is untreated, and coupon 6 was treated. In the table, we give the open-circuit voltages measured under a solar simulator for one cell from each coupon. Due to the resistance of the semi-transparent back contact, the fill factors and solar cell efficiencies are fairly low, and we will not report them here. We also give the four parameters obtained in time-of-flight measurements on each cell: the drift mobilities and the deep-trapping mobility-lifetime products for electrons and for holes.

For time-of-flight measurements, we reduced the sample area by scribing small squares through the  $\text{CdS}/\text{CdTe}$  films to give areas of about  $10^{-2} \text{ cm}^2$ . Dark capacitance measurements (see supplementary materials<sup>15</sup>) indicated that the untreated cells were fully depleted at zero and reverse bias voltages. Treated cells were not fully depleted, and a Mott-Schottky analysis<sup>16</sup> accounted for capacitance measurements.

Time-of-flight (TOF) measures a transit time  $t_T$  for an initial distribution of photocarriers to be displaced a distance  $L$  under the applied voltage  $V$ .<sup>17</sup> We choose  $L$  to be  $d/2$ , where  $d$  is the thickness of the  $\text{CdTe}$  layer. For an initial photocarrier distribution that is close to one contact,  $L = d/2$  corresponds to collection of half of the total photogenerated charge  $Q_0$  in the external circuit. TOF measurements were done using a pulsed diode laser with 660 nm wavelength, which is absorbed within about  $0.25 \mu\text{m}$  in  $\text{CdTe}$ .<sup>18</sup> Hole mobilities are measured using front (glass) side illumination; electrons were measured using back illumination. The laser pulse width was about 4 ns, which is much shorter than the product  $RC$  of the scribed cell's capacitance  $C$  and the series resistance  $R$ , which includes the  $50 \Omega$  electronics. The measured rise time  $t_{RC}$  for a 50% charge response to a fast electronic step was about 40 ns in the small scribed cells.

Fig. 2 presents the graphs for a cell from the untreated coupon 5; in this cell the electric field under reverse bias was fairly uniform across the  $\text{CdTe}$  film. Fig. 2(a) shows the hole photocharge transients  $Q(t)$  at four voltages using front illumination; the photocurrent transient  $i(t)$  was recorded and integrated to obtain  $Q(t)$ . The bias voltage pulses were 1.0 ms long and were applied  $50 \mu\text{s}$  before the laser pulse. With a voltage of  $-1.0 \text{ V}$ , the photocharge collected in  $1.0 \mu\text{s}$  is about 5.1 pC, which we equate to the total charge  $Q_0$  of holes photogenerated in the  $\text{CdTe}$  film by the laser pulse. At smaller field magnitudes charge collection within  $1.0 \mu\text{s}$  is incomplete. This behavior is common in

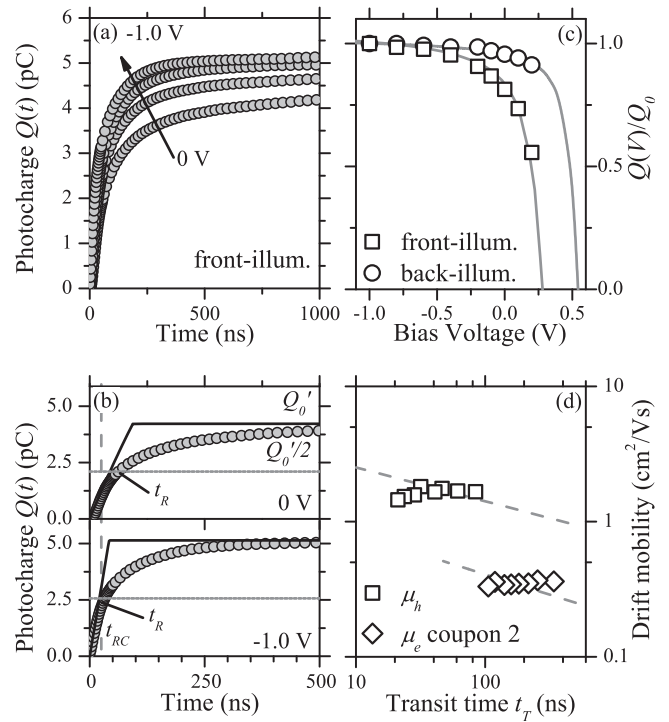


FIG. 2. Time-of-flight measurement at 293 K on a cell from coupon 5 (untreated). (a) Photocharge transients  $Q(t)$  for front illumination (through the glass substrate) using a 4 ns laser pulse (660 nm wavelength). Results are shown for several bias voltages. (b) Photocharge transients along with the electronic risetime  $t_{RC}$  (vertical gray line). The solid lines show the constant drift-velocity model predictions corresponding to the transit times  $t_T$  calculated for each transient. (c) Photocharge collected in  $1 \mu\text{s}$  as a function of bias voltage with front and back illumination (holes and electrons). Open squares are for the hole measurements and open circles are for electron measurements. The solid lines are fits to the Hecht formula for deep-trapping. (d) Drift mobilities for holes from coupon 5 and electrons for coupon 2 calculated from the transit times at different bias voltages. The dashed lines show the prediction of a dispersion model  $\alpha = 0.75$  for the hole mobility of coupon 5 and  $\alpha = 0.70$  for electron mobility of coupon 2.

time-of-flight measurements<sup>19</sup> and is attributed to deep trapping of carriers by defects during their transit.

Fig. 2(b) shows the analysis of these transients to obtain a transit time  $t_T$  for the photocarriers to drift halfway across the sample. This “half collection” definition of  $t_T$  is unusual in single crystal work but is common in less ordered materials. The rise time  $t_R$  is the time required for the transient to reach 50% of its ultimate charge. To calculate the transit time  $t_T$ , we corrected for the electrical response time  $t_{RC}$  using the approximation  $t_T^2 = t_R^2 - t_{RC}^2$ .<sup>19</sup> The vertical dashed lines in Fig. 2(b) indicate the measured value  $t_{RC} = 40 \text{ ns}$ .

The solid lines in Fig. 2(b) are calculations of charge transients that correspond to these transit times  $t_T$  and to the assumption that the initial photocharge distribution moves at a constant drift-velocity after photogeneration at time  $t = 0$ . The photocharge expression is then<sup>19</sup>

$$Q(t) = Q_0 \left( \frac{\tau_t}{2t_T} \right) \left[ 1 - \exp\left(-\frac{t}{\tau_t}\right) \right] \quad \text{for } t \leq 2t_T, \quad (1)$$

where  $d$  is the layer thickness and  $\tau_t$  is a deep-trapping lifetime.

The data taken at  $-1.0 \text{ V}$  are not affected significantly by deep-trapping ( $\tau_t \gg t_T$ ), and they show clearly that the

photocharge collection is more spread out than predicted by the constant drift velocity model. The same conclusion applies at 0 V, although it is obscured somewhat by deep-trapping. We measured similar effects for both electrons and holes in all cells studied. We will return to this apparent spread in transit times shortly.

In Fig. 2(c), the open squares show the total hole photocharge  $Q(V)$  collected at  $1 \mu\text{s}$  as a function of the bias voltage  $V$ . The charge measurements are normalized by the value at  $-1.0 \text{ V}$ , which we equate with  $Q_0$ . As the voltage increases, and the magnitude of the electric field diminishes, the charge  $Q(V)$  falls. We attribute this effect to “deep trapping” of the holes. The solid lines are fits to the Hecht equation<sup>20</sup>

$$\frac{Q(V)}{Q_0} = \frac{\mu\tau_i(V_0 - V)}{d^2} \left[ 1 - \exp\left(-\frac{d^2}{\mu\tau_i(V_0 - V)}\right) \right], \quad (2)$$

where  $d$  is the thickness of the CdTe layer.  $\mu\tau_i$  is a mobility-lifetime product for deep-trapping; it is not a recombination  $\mu\tau$ -product.  $V_0$  is related to the built-in electric field but is not the true built-in potential of the cell. From the fittings, the  $\mu\tau_i$  product for the holes in this cell is  $5.8 \times 10^{-7} \text{ cm}^2/\text{V}$ , and for electrons it is  $1.1 \times 10^{-6} \text{ cm}^2/\text{V}$ . In Table I, we present the Hecht fitting parameters for one cell from each of the six coupons used in this work.

We used the values of  $V_0$  from the Hecht analysis to calculate drift-mobilities for the electrons and holes using the expression

$$\mu_d = \frac{d^2}{2(V_0 - V)t_T}. \quad (3)$$

In Fig. 2(d), we present these drift-mobility estimates as a function of the half-collection transit time, which varies with the electric field across the CdTe layer. We show the hole results for coupon 5 and the electron results for coupon 2; the photocharge transients used to calculate these mobilities are given in the supplementary material.<sup>15</sup> There is little variation with electric field; the mobility values in Figs. 1 and 3, and Table I are from linear fits to the transit time—voltage relation assuming a constant mobility.

We now return to the apparent spread of transit times in Fig. 2(b). “Dispersion,”<sup>21</sup> which is commonly used to

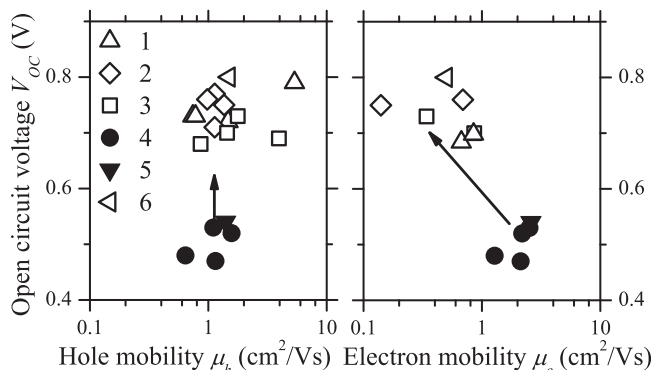


FIG. 3. Correlation of the electron and hole mobilities vs open circuit voltage under solar simulator illumination. The different symbols indicate different coupons. The solid symbols represent measurements on untreated coupons; the open symbols are for coupons following treatment.

interpret drift-mobility measurements in non-crystalline semiconductors, is a possible explanation.<sup>17,22,23</sup> In hydrogenated amorphous silicon and related materials, dispersion results from multiple-trapping in an exponential bandtail of localized electronic states lying just beyond the band edges. As discussed in the supplementary material,<sup>15</sup> dispersion can account for the form of the photocharge transients (cf. Fig. 2(b)). However, dispersion also implies an intrinsic, power-law dependence of the drift-mobility upon the typical transit time  $t_T$ ; these predictions are shown as the dashed lines in Fig. 2(d). We do not see the predicted dependence of the mobility upon the transit time, and we therefore exclude this mechanism.

We speculate that lateral variation of the drift mobility, presumably from crystallite to crystallite, is the reason for the spread of transit times. This mechanism is broadly consistent with previous work on micro-uniformity of CdTe cells and films, which shows significant lateral variation in quantum efficiency and photoluminescence lifetime.<sup>2,24</sup>

The time-of-flight procedures described above worked well for all cells excepting for the electron measurements on coupon 6. These cells had strong trapping near the back interface. To obtain electron drift mobilities in these cells, we used transients recorded using an 850 nm wavelength laser diode, which is weakly absorbed throughout the CdTe film, as well as the hole transient obtained with front illumination and the 660 nm laser. The details of this more complex procedure were published previously.<sup>25</sup>

In Fig. 3, we show the correlation of the open-circuit voltages  $V_{OC}$  with the hole and electron drift mobilities. There is no clear relationship of the hole drift mobility to  $V_{OC}$ , but for the electron drift mobility there is a negative correlation: untreated cells with lower  $V_{OC}$  correspond to larger values of the electron drift mobility than do the treated, higher  $V_{OC}$  cells.

We speculate that the change in the electron drift mobility with treatment reflects a change in the conduction band edge, which is consistent with previously reported effects of post-deposition treatments on the interband absorption spectrum of thin films of CdTe.<sup>26</sup> Presumably, the treatment has relatively little effect on the valence band edge, although we do not understand why the valence band edge would be less sensitive to treatment than the conduction band edge.  $V_{OC}$  is mainly influenced by electron-hole recombination processes, which are greatly suppressed by  $\text{CdCl}_2$  treatment. While mobilities are not expected to affect  $V_{OC}$  directly, when recombination is diffusion-limited the lifetime increases as the minority carrier mobility shrinks.<sup>13,14</sup>

Takahashi *et al.*<sup>4</sup> studied Schottky diodes based on electrodeposited CdTe films. Their values of the electron and hole drift mobilities were about  $2 \times 10^1 \text{ cm}^2/\text{V s}$ , which are somewhat larger than our values. Their results appear reasonably consistent with the present measurements, given the differences in the films. Gilmore *et al.* reported a strong effect of illumination on the Hall effect of their undoped CdTe films<sup>9</sup> and inferred an intragrain electron mobility of about  $3 \times 10^2 \text{ cm}^2/\text{V s}$ . Our time-of-flight results do not seem compatible with theirs, but there are substantial differences between the experiments. Hall effect measurements are done with transport parallel to the substrate of simple films,

whereas the drift mobilities are measured normal to the substrate in multilayer photodiode structures. Previous authors have generally attributed the reduction in drift-mobilities of thin films compared with single crystals to grain boundary effects. The grains in thin films used for contemporary solar cells are fairly large and can extend through the CdTe layer,<sup>2</sup> so in the drift mobility experiments reported here the effects of traversing grain boundary should be minor. We therefore favor microscopic mechanisms for mobility reduction over more macroscopic mechanisms such as grain boundaries. Such microscopic mechanisms would be effective within each crystallite; electrostatic fluctuations due to charged defects, dislocations, and chemical disorder of vacancies, interstitials, etc., are possibilities. These broad speculations do not address the interesting feature that, relative to crystalline values, the electron mobility is reduced more in the polycrystalline thin films than is the hole mobility. We do note that the effects of disorder on electron and hole drift mobilities in hydrogenated amorphous silicon are also very different.<sup>23</sup>

In Table I, we report deep-trapping mobility-lifetime products for both electrons and holes. There have been many previous studies of trapping in CdTe solar cells with deep level transient spectroscopy (DLTS) and other methods.<sup>27</sup> These typically report the location of the trap level within the energy gap, but not mobility-lifetime products. One transient photoconductivity measurement has been reported showing a 6  $\mu$ s lifetime for holes;<sup>28</sup> this is consistent with the deep-trapping lifetime in the present work, which is about 1  $\mu$ s for holes. Deep trapping mobility-lifetime products have been reported for single crystal CdTe detectors.<sup>5</sup> The values from these measurements are around  $8 \times 10^{-4}$  cm<sup>2</sup>/V for electrons and  $7 \times 10^{-5}$  cm<sup>2</sup>/V for holes, which are much larger than our measurements. The present mobility-lifetime products can also be converted into a trapping diffusion length  $L_t = \sqrt{(kT/e)\mu\tau}$ , where  $kT/e$  is the ratio of the thermal energy  $kT$  to the electron charge. The range in Table I then yields  $L_t$  values from 0.7 to 3  $\mu$ m at room temperature. This is reasonably consistent with diffusion lengths reported from electron beam-induced current (EBIC) measurements<sup>29</sup> and from cathodoluminescence measurements.<sup>30</sup>

We now turn to the fact that the electron transit times reported here are hundreds of times longer than time-resolved photoluminescence lifetimes for cells with comparable  $V_{OC}$  values.<sup>31</sup> The photoluminescence lifetimes are nanoseconds or less and have commonly been identified with the minority carrier (electron) recombination lifetime; for a recent review, see Ref. 28. Our transit times are for electrons traversing the film's entire thickness, but most photoluminescence lifetime measurements involve radiative recombination of photocarriers close to the CdS/CdTe interface. This appears to leave open the possibility of extremely different material properties between and bulk and the interface, but recent two-photon measurements of luminescence lifetimes largely rule this out.<sup>32</sup> The fact that drift mobilities are fairly low in thin film CdTe suggests to us that the fast luminescence lifetimes may probe an exciton dissociation process instead of the ultimate photocarrier recombination process,

which is the interpretation commonly applied to low mobility organic solar cell materials.<sup>33</sup>

This research was partly supported by the National Science Foundation (CBET-1336147). The authors thank Gang Xiong for discussions.

- <sup>1</sup>M. A. Green, K. Emery, Y. Hishikawa, W. Warta, and E. D. Dunlop, *Prog. Photovolt. Res. Appl.* **22**, 701 (2014).
- <sup>2</sup>B. E. McCandless and J. R. Sites, in *Handbook of Photovoltaic Science and Engineering*, 2nd ed., edited by A. Luque and S. Hegedus (John Wiley & Sons, New York, 2011), p. 600.
- <sup>3</sup>R. Scheer and H.-W. Schock, in *Chalcogenide Photovoltaics: Physics, Technologies, and Thin Film Devices* (John Wiley & Sons, 2011), p. 4.1.3.
- <sup>4</sup>M. Takahashi, K. Uosaki, H. Kita, and S. Yamaguchi, *J. Appl. Phys.* **60**, 2046 (1986).
- <sup>5</sup>P. J. Sellin, A. W. Davies, A. Lohstroh, M. E. Özsan, and J. Parkin, *IEEE Trans. Nucl. Sci.* **52**, 3074 (2005).
- <sup>6</sup>K. Suzuki, S. Seto, T. Sawada, and K. Imai, *IEEE Trans. Nucl. Sci.* **49**, 1287 (2002).
- <sup>7</sup>J. Osenzweig, M. Adolf, H. Dignus, and U. Birkholz, *Nucl. Instrum. Methods Phys. Res.* **283**, 255 (1989).
- <sup>8</sup>C. Canali, M. A. Nicolet, and J. W. Mayer, *Solid-State Electron.* **18**, 871 (1975).
- <sup>9</sup>A. S. Gilmore, V. Kaydanov, T. R. Ohno, D. Grecu, and D. Rose, in *II-IV Compound Semiconductor Photovoltaic Materials*, edited by R. W. Birkmire, R. Noufi, D. Lincot, and H. Shock (Mater. Res. Soc. Symp. Proc., 2001), vol. **668**, p. H510.1.
- <sup>10</sup>M. Gloeckler, A. L. Fahrenbruch, and J. R. Sites, in *3rd World Conference on Photovoltaic Energy Conversion, Osaka* (2003), p. 491.
- <sup>11</sup>E. A. Schiff, *Sol. Energy Mater. Sol. Cells* **78**, 567 (2003).
- <sup>12</sup>Q. Long, S. A. Dinca, D. A. Goldman, E. A. Schiff, J. Theil, and M. Yu, in *Proceedings of the 40th IEEE Photovoltaic Specialists Conference, Denver* (2014).
- <sup>13</sup>D. R. Wight, I. D. Blenkinsop, W. Harding, and B. Hamilton, *Phys. Rev. B* **23**, 5495 (1981).
- <sup>14</sup>M. D. Abbott, R. A. Bardos, T. Trupke, K. C. Fisher, and E. Pink, *J. Appl. Phys.* **102**, 044502 (2007).
- <sup>15</sup>See supplementary material at <http://dx.doi.org/10.1063/1.4891846> for dark capacitance measurements and a discussion of dispersive transport.
- <sup>16</sup>S. M. Sze, in *Semiconductor Devices: Physics and Technology*, 2nd ed. (John Wiley & Sons, Inc., New York, 2001), p. 101.
- <sup>17</sup>Q. Wang, H. Antoniadis, and E. A. Schiff, *Phys. Rev. B* **47**, 9435 (1993).
- <sup>18</sup>T. H. Myers, S. W. Edwards, and J. F. Schetzina, *J. Appl. Phys.* **52**, 4231 (1981).
- <sup>19</sup>S. A. Dinca, E. A. Schiff, B. Egaas, R. Noufi, D. L. Young, and W. N. Shafarman, *Phys. Rev. B* **80**, 235201 (2009).
- <sup>20</sup>K. Hecht, *Zeits. Phys.* **77**, 235 (1932).
- <sup>21</sup>H. Scher and E. M. Montroll, *Phys. Rev. B* **12**, 2455 (1975).
- <sup>22</sup>V. Coropceanu, J. Cornil, D. A. da Silva Filho, Y. Olivier, R. Silbey, and J.-L. Bredas, *Chem. Rev.* **107**, 926 (2007).
- <sup>23</sup>E. A. Schiff, *J. Phys. Condens. Matter* **16**, S5265 (2004).
- <sup>24</sup>C. Kraft, H. Hempel, V. Buschmann, T. Siebert, C. Heisler, W. Wesch, and C. Ronning, *J. Appl. Phys.* **113**, 124510 (2013).
- <sup>25</sup>S. A. Dinca, E. A. Schiff, W. N. Shafarman, B. Egaas, R. Noufi, and D. L. Young, *Appl. Phys. Lett.* **100**, 103901 (2012).
- <sup>26</sup>B. E. McCandless, L. V. Moulton, and R. W. Birkmire, *Prog. Photovolt. Res. Appl.* **5**, 249 (1997).
- <sup>27</sup>A. Balcioglu, R. K. Ahrenkiel, and F. Hasoon, *J. Appl. Phys.* **88**, 7175 (2000).
- <sup>28</sup>R. K. Ahrenkiel, N. Call, S. W. Johnston, and W. K. Metzger, *Sol. Energy Mater. Sol. Cells* **94**, 2197 (2010).
- <sup>29</sup>S. A. Galloway, P. R. Edwards, and K. Durose, *Sol. Energy Mater. Sol. Cells* **57**, 61 (1999).
- <sup>30</sup>M. J. Romero, T. A. Gessert, and M. M. Al-Jassim, *Appl. Phys. Lett.* **81**, 3161 (2002).
- <sup>31</sup>W. K. Metzger, D. Albin, D. Levi, P. Sheldon, X. Li, B. M. Keyes, and R. K. Ahrenkiel, *J. Appl. Phys.* **94**, 3549 (2003).
- <sup>32</sup>D. Kuciauskas, A. Jabevece, J. M. Burst, J. N. Duenow, R. Chere, D. H. Levi, and R. K. Ahrenkiel, *IEEE J. Photovolt.* **3**, 1319 (2013).
- <sup>33</sup>P. E. Shaw, A. Ruseckas, and I. D. W. Samuel, *Adv. Mater.* **20**, 3516 (2008).

# Electron and hole drift mobility measurements on thin film CdTe solar cells (Supplementary materials)

Qi Long<sup>1</sup>, Steluta A. Dinca<sup>1</sup>, E. A. Schiff<sup>1</sup>, Ming Yu<sup>2</sup>, and Jeremy Theil<sup>2</sup>

<sup>1</sup>Department of Physics, Syracuse University, Syracuse, 13244, United States

<sup>2</sup>First Solar Inc., Santa Clara, United States

## CAPACITANCE MEASUREMENTS

For all cells we measured the room-temperature capacitance at 1 kHz. We have graphed results for the six coupons at room temperature in Fig. S1 using the form suggested by the Schottky analysis<sup>1</sup>:

$$\left(\frac{A}{C}\right)^2 = \frac{2(V_0 - V)}{e\epsilon\epsilon_0 N_A}, \quad (1)$$

where  $N_A$  is the acceptor doping level,  $\epsilon$  is the relative dielectric constant, and  $V_0$  is nominally the built-in potential. The capacitance for the untreated samples shows only a small change with the reverse bias, which indicates nearly full depletion even

at short circuit. For the cell from coupon 5, we also show the geometrical capacitance expected from a profilometer measurement, which agrees well with the capacitance measurements under -2 V of reverse bias.

## DISPERSIVE TRANSPORT

In this section we briefly review the main features of “dispersive transport”. We illustrate how the dispersive form can be fitted to the photocharge transients that we measure, and we present the dispersive relationship between the drift-mobility and the transit time.

The drift mobility  $\mu_d$  is defined as:

$$\mu_d \equiv L/Et_T \quad (2)$$

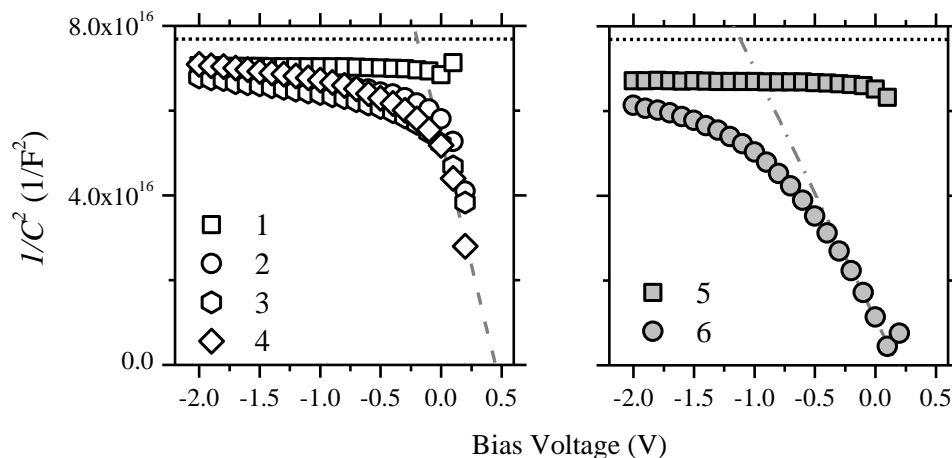


Fig. S1. Dark capacitance measurements ( $10^3$  Hz) on cells from all six coupons. Coupon 1 and 5 are untreated, the remaining coupons received post deposition treatments. We illustrate the Schottky model fits for the cells from coupons 4 and 6.

where  $E$  is the electric field magnitude and  $L$  is the displacement of the photocarrier distribution following photogeneration at time  $t = 0$ . In this paper we've defined the transit time  $t_T$  as corresponding to a displacement of half the thickness  $d$  of the CdTe layer, so  $L = d/2$ . This transit time corresponds to collection of half of the total charge  $Q_0$  in the external bias circuit. For ordinary transport with a constant drift-velocity, and neglecting deep-trapping, we can write  $Q(t)$  as:

$$Q(t) = \begin{cases} \frac{Q_0}{2t_T} t, & t < 2t_T \\ Q_0, & t \geq 2t_T \end{cases} \quad (3)$$

In Fig. S2, we show the photocharge transient of a cell from coupon 5 at -1.0V bias along with the non-dispersive form of equation (3) with the same transit time. We can see the fitting for non-dispersive transport doesn't fit the photocharge well, especially for times longer than the transit time. We chose the -1.0 V transient for illustrative purposes because the deep trapping time of about 400 ns does not noticeably affect the photocharge transient.

We examined the possibility that the slow collection of the photocharge corresponds to the dispersive transport model.<sup>2</sup> For the dispersive case, the photocurrent transient is written:

$$i(t) = \begin{cases} i_0 (t/t_T)^{-1+\alpha}, & t < t_T \\ i_0 (t/t_T)^{-1-\alpha}, & t \geq t_T \end{cases} \quad (4)$$

where  $\alpha$  is the dispersion parameter and  $t_T$  is the transit time. With dispersive transport, the power law for the photocurrent decay changes at  $t_T$ . The current prefactor  $i_0 = \alpha Q_0 / (2t_T)$ , where  $Q_0$  is defined as the photocharge collected at long times by integration of the photocurrent. The corresponding photocharge transient is:

$$Q(t) = \begin{cases} \frac{Q_0}{2} (t/t_T)^\alpha, & t < t_T \\ Q_0 \left[ 1 - \frac{1}{2} (t/t_T)^{-\alpha} \right], & t \geq t_T \end{cases} \quad (5)$$

Note that the transit time still corresponds to collection of half the photocharge  $Q_0/2$ . The curved line in Fig. S2 compares this form to a CdTe hole transient (front illumination) using  $\alpha=0.75$ . Note that the measured data are slowed somewhat by an electronic risetime of about 40 ns. The fitting gives a reasonable account for the photocharge transient.

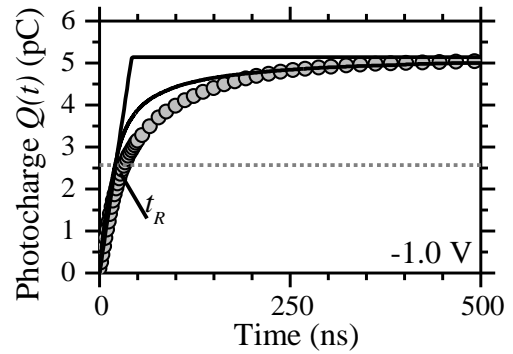


Fig. S2. Transient photocharge for coupon 5 at -1.0V. The straight line shows the fitting for non-dispersive model and the curved line shows the fitting for dispersion model with  $\alpha=0.75$ .

An important feature of dispersive transport is that the drift mobility depends upon the transit time. The drift mobility  $\mu_D$  is:

$$\mu_D \equiv \frac{d^2}{2Vt_T} = \frac{\mu_0}{\alpha} (vt_T)^{\alpha-1}, \quad (6)$$

where  $d$  is the thickness of the sample and  $V$  is the voltage across the sample. Eq. (6) was used to calculate the dispersive curves used in Fig. 2(d) of the letter. We did not include deep-trapping in these calculations. The transit times are all much shorter than the times at which deep-trapping would significantly affect dispersive transients.

We emphasize that dispersion does not imply a nonlinear field-dependence to the photocurrents; prior to transit, the average displacement of a photocarrier distribution photogenerated at time  $t = 0$  remains proportional to the electric field.  $\mu_0$  and  $\nu$  are parameters whose physical significance depends upon the microscopic mechanism underlying the dispersion. Thus in the exponential bandtail multiple-trapping model, they are the band mobility and the trap attempt-to-escape frequency, respectively<sup>3</sup>. The hallmark of this multiple-trapping model is the temperature dependence of the dispersion parameter  $\alpha = kT/\Delta E$ , where  $kT$  is the thermal energy and  $\Delta E$  is the width of the exponential bandtail.

### PHOTOCHARGE TRANSIENTS FOR ELECTRONS

Fig. S3 below shows the photocharge transients measured at several voltages using rear illumination and a 660 nm laser wavelength. The transients are dominated by electron transport. As can be seen in Fig. S1, the capacitance measurements do indicate some dark space charge in the sample. It was especially noticeable for the cell from coupon 6. This leads to some nonuniformity in the electric field. In addition, deep-trapping modifies the simple equation of the transit time with the photocharge risetime. We have discussed both of these effects in previous work; see appendix B of ref.<sup>4</sup>. In the present work, we neglected these effects, which are smaller than the effects of a distribution of transit times.

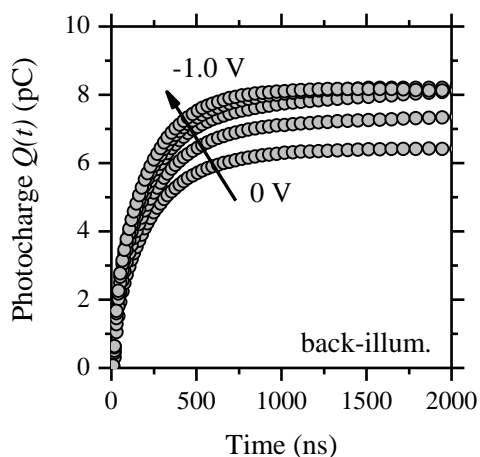


Fig. S3: Transient photocharge measurements following a 4 ns laser pulse (660 nm wavelength) through the back contact of a cell from coupon 2. The pulsed bias voltages were 0, -0.2, -0.6, -0.8, and -1.0 V.

## REFERENCES

- <sup>1</sup> S. M. Sze, in *Semiconductor Devices: Physics and Technology*, 2<sup>nd</sup> edition, (John Wiley & Sons, Inc., New York, 2001), p. 101.
- <sup>2</sup> H. Scher and E. M. Montroll, *Phys. Rev. B*, **12**, 2455 (1975).
- <sup>3</sup> Q. Wang, H. Antoniadis and E. A. Schiff, *Phys. Rev. B*, **47**, 9435 (1993).
- <sup>4</sup> S. A. Dinca, E. A. Schiff, B. Egaas, R. Noufi, D. L. Young and W. N. Shafarman, *Phys. Rev. B*, **80**, 235201-1 (2009).